

# AN EMITTANCE ALGORITHM FOR A HIGH-INTENSITY LOW-EMITTANCE BEAM \*

E. Lessner<sup>†</sup> and J.W. Lewellen

Advanced Photon Source, Argonne National Laboratory, Argonne, IL

## Abstract

The Advanced Photon Source (APS) linac together with a photocathode rf gun is the source for a self-amplified spontaneous emission (SASE) free-electron laser (FEL). For optimal performance the APS SASE FEL requires a low-emittance high-intensity electron beam. A three-screen measurement section, located upstream of the Low-Energy Undulator Test Line, where the SASE FEL is located, allows monitoring of the beam emittance. Control and reduction of the emittance growth is achieved experimentally by various methods such as steering or adjusting the rf phases of one or more klystrons along the linac. In particular, emittance growth caused by transverse wakefields can be reduced by strategically placing local trajectory distortions. The factors and methods affecting the beam projection at each of the three screens are systematically investigated using simulations. The results will be used to create an algorithm that allows an effective and systematic means to reduce beam distortions at the end of the linac. Initial experimental results are presented.

## 1 OVERVIEW

The electron beam delivered by the Advanced Photon Source (APS) linac to the Low-Energy Undulator Test Line (LEUTL) free electron laser (FEL) must maintain small normalized emittance, low energy spread, high peak current, and high stability [1]. In this paper, we present the initial results of a comprehensive study of errors affecting the electron beam qualities in the linac and means to mitigate their effects. The objective is to produce an algorithm to perform systematic and effective corrections of the beam distortions prior to its delivery to the FEL.

The linac proper consists of five sections, designated by L1 to L5. The photoinjector, L1, consists of a photocathode gun with emittance compensation solenoid and one 3-m S-band traveling-wave (TW) accelerating structure. The gun is a standard 1.6-cell, 'Gun-IV' variant of the basic SLAC/BNL/UCLA design. L2, L4, and L5 sections contain four 3-m TW accelerating structures each. L3 contains a bunch compressor system [2] that provides peak currents of  $\geq 300$  A. The system comprises a four-magnet chicane, quadrupoles, and diagnostics for emittance measurement and coherent synchrotron radiation characterization. A second three-screen emittance measurement section is placed at the end of a 20-m-long

transport line following the linac. We will refer to this system as the PAR-Bypass system (PBS).

Factors such as rf voltage and phase jitter, magnet strength errors, and misalignments of magnetic components can degrade the linac beam quality. In particular, high peak currents can produce strong wakefields that corrupt the beam parameters. Longitudinal wakefields can be corrected by appropriate phasing of the rf voltage, e.g., by placing the beam behind crest, mitigating head-tail effects but also reducing the acceleration gradient. Transverse wakefields can be reduced by keeping the beam centered in the accelerating structures along the line. In earlier work we examined in detail the effects of transverse wakefields due to various sources of errors, such as consecutive-cell misalignments in a single accelerating structure and alignment errors between the structures [3] and shown that the latter are the most detrimental, causing emittance dilution and beam losses due to large beam-centroid excursions. In that work we showed that appropriately placed "emittance-bumps" can restore the normalized emittance to specifications and minimize the centroid offsets before the FEL line. In this paper we explore the technique in a systematic way, by sweeping, through simulations, the entire post-injector linac to find the optimum placement and magnitude of the bumps for a specific error. The simulation results are shown to be in good agreement with preliminary experimental tests.

## 2 SIMULATIONS

We use the program "elegant" [4] to transport the beam from after the first accelerating structure to the PBS. Simulations of the photoinjector are done by PARMELA [5] and the resulting beam distribution is input to "elegant." Effects of random alignment errors between structures are simulated by wakefield dipole mode. In our simulations, we chose a 300-A-peak-current lattice out of the various lattices modeled in reference [6]. The PARMELA beam contains 1 nC of charge, at 25 MeV, and has a normalized emittance of about 5 mm mrad.

Figure 1 shows the lattice functions from L2 to PBS, where diamonds depict dipole corrector locations and crosses indicate beam position monitors (BPM). As a preliminary step, transverse wakefields at various amplitude levels were simulated to induce significant emittance growth while avoiding beam losses due to centroid excursions. For the purposes of this paper we restricted the misalignments to the vertical direction. We found that random vertical misalignments of 400  $\mu\text{m}$  rms cause an emittance dilution of 25% and no losses other

\* Work supported by the U.S. Department of Energy, Office of Basic Energy Sciences under Contract No. W-31-109-ENG-38.

<sup>†</sup> esl@aps.anl.gov

than those suffered by the ideal model at the bunch compressor, on the order of 10%. We then proceeded to systematically place closed bumps along the linac according to the following algorithm. First, we simulated single four-magnet bumps and required “elegant” to find, by optimization, the corrector strengths necessary to restore the nominal normalized emittance and centroid offsets at the first PBS screen. For each set of four magnets, the strength of the first selected magnet was varied from -2 mrad to 2 mrad.

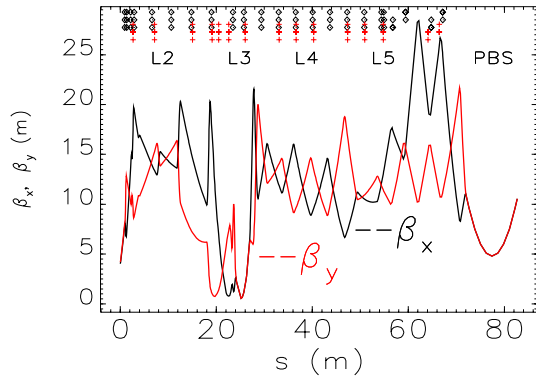


Figure 1: Horizontal and vertical beta functions of the linac lattice model. Diamonds indicate correctors and crosses indicate BPM locations.

In all simulated cases there were losses, except when the first magnet in the bump had negligible strength, which led us to study three-magnet bumps. For the most effective three-magnet bump case, the centroid displacement at the first PBS screen was  $\approx 500 \mu\text{m}$ , with some centroid excursions as high as 3 mm. The required corrector strengths were between +3 mrad and -3 mrad.

Next, we investigated the use of two closed bumps at opposite sides of the bunch compressor, since the first studies showed that bumps near the compressor system were quite damaging to the beam. The optimization procedure followed the same guidelines as before, but was applied in two stages. First, we selected sets of correctors in L1 and L2, and required the nominal emittance value at the end of L2, together with zero centroid offset. After the “best” bump was found, we searched L4 and L5 correctors to form an additional bump. As expected, bumps formed by correctors in the transport line after L5 proved to be ineffective in correcting the emittance and centroid at the first PBS screen.

In Fig. 2(a) we compare the emittance from the most effective two-bump, three-magnet system simulation to the “best” one-bump case, together with the emittance dilution caused by the vertical wakefield distortions and the unperturbed emittance. Figure 2(b) shows the corresponding centroid excursions. Although the bumped centroid displacement is close to 1 mm in L2, in the two-bump model, the centroid is corrected before entering L3, and does not degrade the compressor output beam. The two-bump method also has the advantage of requiring much smaller corrector strengths than the one-bump

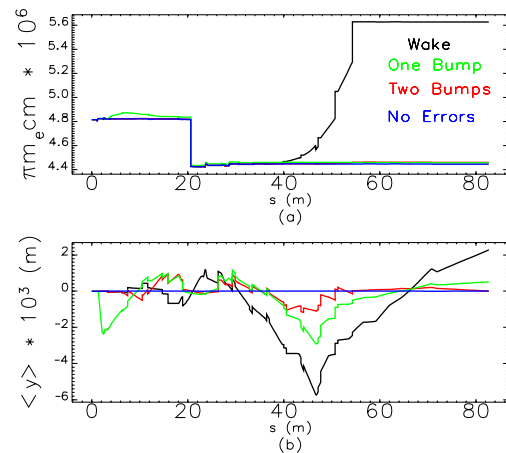


Figure 2: Comparison of normalized emittance (a) and centroid excursions (b) after “one-bump” and “two-bumps” emittance correction. The unperturbed and wakefield-distorted data are shown for reference.

method, on the order of 1 mrad or less.

Figure 3 shows the simulated beam images at three PBS screens, where the wakefield-induced beam enlargements and offsets are clearly seen. The upper plots show the unperturbed beam. The wake-perturbed beam and the bump-corrected beam images are shown in the middle and lower plots, respectively.

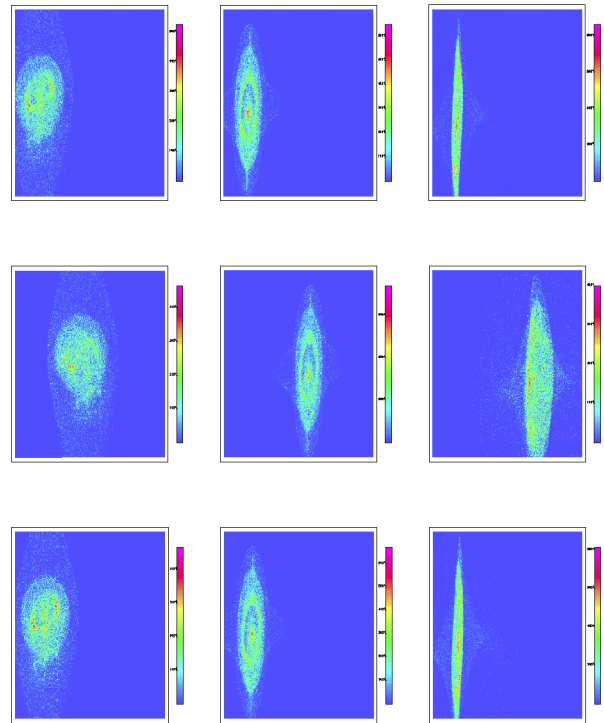


Figure 3: The unperturbed, wakefield-distorted beam, and the two-bump-corrected beam images at the three PBS screens. The vertical beam size is along the x-axis.

The unperturbed vertical beam size was recovered after the two-bump correction. In Fig. 4, we show the unperturbed, perturbed, and corrected distributions at the

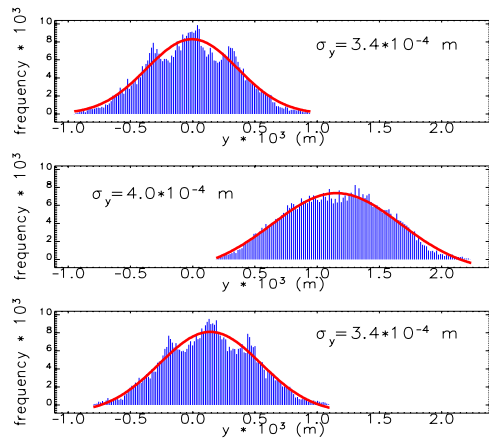


Figure 4: Comparison of the unperturbed, perturbed, and corrected vertical projections of the beam distribution at the first screen. The smooth curves represent Gaussian fits.

first PBS screen. A Gaussian fit is superimposed on the projected distributions. The two-bump-corrected distribution  $\sigma_y$  reproduces the unperturbed distribution  $\sigma_y$ .

### 3 EXPERIMENTAL TEST

Our initial tests were carried out under conditions somewhat different from those in the simulation. The main difference was the use of a lower,  $\approx 100$  pC, beam charge, due to drive laser and photocathode quantum efficiency problems. We also were running without compression to help eliminate any effects from rf phase jitter; since the klystron voltage is automatically scaled to maintain a consistent rate of energy gain, this does not impact the magnetic lattice.

The linac trajectory feedback system operates on the beam position monitor (BPM) error signal calculation, which has a functional equation as follows:

$$R + \Delta - P_{des} = E. \quad (1)$$

where  $R$  is the raw signal,  $\Delta$  is the BPM offset,  $P_{des}$  is the desired position, and  $E$  is the resulting error signal. This allows us to adjust for electronic or physical BPM offsets without influencing the desired beam position setpoints. Since both  $\Delta$  and  $P_{des}$  are adjustable by an experimenter, the APS linac BPM system provides a natural method for simulating both structure offsets and corrections.

The measurement began by establishing a nominal “good” trajectory to the PAR-Bypass region and obtaining a good match to the design beam parameters. All values of  $\Delta$  were set to zero (which is their usual setting in operation), and  $P_{des}$  was set to the raw signal values to load the starting nominal trajectory into the trajectory feedback system.

Next, the prescribed series of “random” misalignments were simulated by adjusting the values of  $\Delta$  at appropriate BPMs. This approach forces the beam trajectory to the desired offsets through the structures while maintaining.

the “appearance” of a good trajectory to the control system. Finally, the prescribed “correction” was applied by altering the BPM desired position setpoints,  $P_{des}$ , at selected locations.

After each step described above, images were captured at the first PBS screen and the vertical spot size measured via whole-image integration (as opposed to lineouts). Since the emittance was measured before the trajectory distortions were applied, and since at these low charges the changing wakes are not significant, we can approximate the change in beam emittance for each of the settings by:

$$\epsilon_{n,d} \approx \epsilon_{n,o} \cdot \frac{\sigma_d^2}{\sigma_o^2}, \quad (2)$$

where  $\epsilon_n$  is the normalized emittance,  $\sigma$  is the measured spot size, and the subscripts “o” and “d” refer to the original and post-orbit-distortion values, respectively. Table 1 lists the results of the measurements. We see that we are able to easily introduce, even at the low initial charge, a large emittance growth and that we are able to recover most of that growth via relatively simple tuning.

Table 1: Results of Beam Orbit Distortion Upon Beam Spot Profile, and Projected Emittance Growth

Measurement	$\sigma$ (pixels)	$\epsilon_n$ ( $\mu\text{m}$ )
Before 1 <sup>st</sup> distortion	19.3	7.0
After 1 <sup>st</sup> distortion	22.8	9.7
After 2 <sup>nd</sup> distortion	22.7	9.7
After correction	20.8	8.1

### 4 SUMMARY

Our future plans include a systematic investigation of rf voltage and phase jitter effects, as well as further refinement of the transverse study. The fair agreement between the experimental test and the simulation results is encouraging and confirms that the linac responds closely to the simulated models derived in reference [6]. It is reasonable to consider an algorithm that allows systematic and as automated as possible corrections to beam distortions, to meet the requirements imposed by optimal FEL performance.

### 5 REFERENCES

- [1] S. Milton et al., “FEL Development at the APS,” Proc. of Free Electron Laser Challenges II (1999).
- [2] M. Borland and J. Lewellen, “Initial Characterization of Coherent Synchrotron Radiation Effects in the APS Bunch Compressor,” these proceedings (2001).
- [3] E. Lessner, “Wakefield Effects in the APS Linac,” Linac Conf Proc. (2000).
- [4] M. Borland, APS LS 287 (2000).
- [5] L.M. Young and J.H. Billen, LAN LA-UR-96-1835 (1996).
- [6] M. Borland et al., “A Highly Flexible Bunch Compressor for the APS Linac,” Linac Conf. Proc. (2000).